Compressed Sensing for Capability Localization in Large Language Models

Anna Bair [1] **Yixuan Even Xu** [1] **Mingjie Sun** [1 2] **Zico Kolter** [1]

Abstract

Large language models (LLMs) exhibit a wide range of capabilities, including mathematical reasoning, code generation, and linguistic behaviors. We show that many capabilities are highly localized to small subsets of attention heads within Transformer architectures. Zeroing out as few as five task-specific heads can degrade performance by up to 65% on standard benchmarks measuring the capability of interest, while largely preserving performance on unrelated tasks. We introduce a compressed sensing based method that exploits the sparsity of these heads to identify them via strategic knockouts and a small number of model evaluations. We validate these findings across Llama and Qwen models ranging from 1B to 8B parameters and a diverse set of capabilities including mathematical abilities and code generation, revealing a modular organization in which specialized capabilities are implemented by sparse, functionally distinct components. Overall, our results suggest that capability localization is a general organizational principle of Transformer language models, with implications for interpretability, model editing, and AI safety. Code is released at `https://github.com/locuslab/llm-components`.

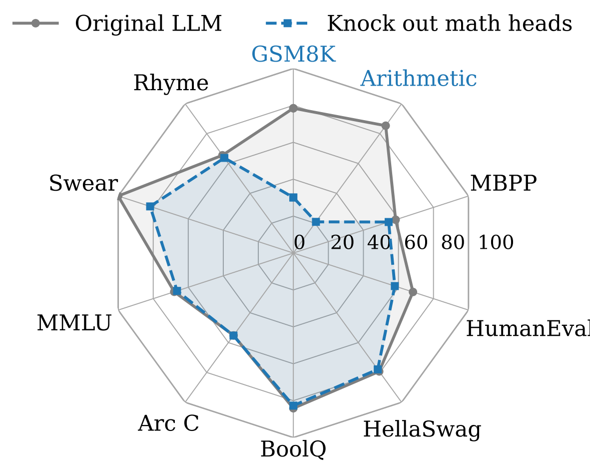

Figure 1. Knocking out the top five math heads identified by our compressed sensing method greatly reduces performance on math datasets (GSM8K and Arithmetic) while leaving other tasks relatively unaffected.

1. Introduction

Understanding how large language models represent and execute diverse capabilities remains a central challenge in AI research. These capabilities, such as mathematical reasoning or code generation, represent higher-level skills that require coordinated computation across multiple model components, rather than simple fact retrieval. We investigate whether task-specific capabilities can be localized to specific components within transformer architectures. Previous work has successfully isolated factual associations to particular neurons and layers (Maini et al., 2023; Meng et al., 2023), raising the question of whether the same principle of localization extends to complex behavioral capabilities. Our central finding is that many capabilities are indeed highly localized, but to sparse sets of attention heads rather than individual neurons.

Similarly to how factual knowledge can be traced to specific model components, we find that task-specific skills are concentrated in small subsets of attention heads. We measure task-specificity by knocking out attention heads, or setting their output to zero, and evaluating the accuracy of the resulting model on the task of interest. A drop in accuracy indicates that the head was responsible for some amount of task-specific computation. Knocking out as few as five task-specific heads causes performance degradations of up to 65% on standard benchmarks measuring the target task while leaving performance on unrelated tasks intact, as shown in Figure 1. This extreme localization suggests that Transformer models organize capabilities in a modular fashion, with different functional specializations handled by distinct computational units.

[1]Carnegie Mellon University [2]Thinking Machines Lab. Correspondence to: Anna Bair <abair@cmu.edu>.

Preprint. February 10, 2026.

A key contribution of our work is the development of efficient algorithms for identifying task-specific heads. While exhaustive greedy search methods involve knocking out each head within a model individually and can thus require thousands of model evaluations, we introduce a novel compressed sensing approach that achieves comparable accuracy with up to $50\times$ fewer evaluations by exploiting the extreme sparsity of task-specific heads.

Compressed sensing is a framework for efficiently reconstructing sparse signals using a small number of linear measurements (Donoho, 2006; Candes & Tao, 2006; Candes & Wakin, 2008). Here, we treat the contribution of each attention head to task performance as a sparse signal and obtain measurements by ablating random subsets of heads and observing the resulting changes in task performance. By solving a sparse regression problem over these measurements, we recover estimates of individual head importance without ever evaluating any heads in isolation. This efficient localization method could open up possibilities for practical applications of capability localization, including targeted model editing and analysis of how models acquire and execute different skills.

In addition to identifying task-specific heads, we present two additional phenomena: universal heads and scale-dependent localization. Universal heads play critical roles across multiple capabilities simultaneously. Ablating these heads causes severe performance degradation on many tasks at once, suggesting that they implement core computations required for general language understanding rather than specialized skills. We also find that capability localization can depend on the scale of the model. Larger models tend to exhibit higher degrees of localization, and in some cases, different types of capabilities emerge at different scales.

2. Related Works

2.1. Attention head functionality

A large body of work investigates the functionality and specialization of attention heads in Transformer models. Much of this research focuses on in-depth analyses of individual heads or narrow capabilities, often aiming to mechanistically explain specific behaviors. Prior approaches can be broadly categorized along two axes: whether they are modeling-free (analyzing a single pretrained model) or require training or comparing multiple models, and whether evaluation relies on mechanistic probes or standard downstream benchmarks (Zheng et al., 2024). Our work adopts a modeling-free, inference-only approach and validates findings using mechanistic interventions and standard task evaluations.

Early studies established that attention heads are often redundant and that only a subset is necessary for strong performance. Voita et al. (2019) showed that retaining a small number of specialized heads is sufficient for machine translation, while Michel et al. (2019) demonstrated substantial redundancy among attention heads in transformers. Clark et al. (2019b) further identified recurring functional patterns among BERT attention heads.

More recent work has identified attention heads associated with specific behaviors and tasks, including induction heads (Olsson et al., 2022), retrieval in long-context settings (Wu et al., 2024; Tang et al., 2024; Xiao et al., 2024), copy suppression (McDougall et al., 2023), in-context learning (Yin & Steinhardt, 2025), arithmetic (Nikankin et al., 2024; Zhang et al., 2024), safety (Zhou et al., 2025), hallucination under false premises (Yuan et al., 2024), syllogistic reasoning (Kim et al., 2025), and knowledge conflict (Jin et al., 2024). These studies often provide detailed mechanistic explanations of individual heads or circuits underlying a particular capability. In contrast, our work aims to complement these efforts by providing a general-purpose method for identifying task-specific heads across a wide range of capabilities, without requiring task-specific model training or deep per-head analysis.

Attention heads have been identified using a variety of techniques. Direct ablation measures the causal impact of removing a head on downstream metrics such as accuracy or output logits (Michel et al., 2019; Zhou et al., 2025). Other approaches analyze similarities or changes in attention head weight matrices to infer specialization (Voita et al., 2019; Chen et al., 2025). Most similar to our work are two recent analyses of task-specific attention heads. Chen et al. (2025) compares attention head weights between a base model and a task-finetuned model to identify heads most affected by finetuning. While this approach directly identifies task-relevant heads, it requires training task-specific models, which our method does not require. Wang et al. (2025) identifies circuits of attention heads responsible for certain tasks, but their emphasis is on developing a finetuning method to increase knowledge flow through these circuits rather than demonstrating the versatility of a localization procedure.

2.2. Fact localization and skill localization

Several works study the localization of factual knowledge or skills within neural networks. Maini et al. (2023) localize memorized training examples in ResNet and ViT models using gradient-based attribution methods. Panigrahi et al. (2023) localize skills by finetuning models on specific NLP tasks, identifying small sets of neurons critical to the learned skill, and demonstrating skill transfer by grafting those neurons into unfinetuned models. These approaches typically rely on training or finetuning models and focus on neuron-level representations.

In contrast, our work focuses on head-level localization in pretrained transformer models and identifies components responsible for executing capabilities rather than storing individual facts or learned parameters from finetuning.

2.3. Mechanistic interpretability

Mechanistic interpretability research aims to uncover how neural networks internally represent and compute meaningful features. The linear representation and superposition hypotheses study how multiple features may be encoded within shared activation spaces (Elhage et al., 2022; Bricken et al., 2023; Templeton et al., 2024), often using sparse autoencoders to extract interpretable features.

Other work has examined the relationship between localization and model editing. Hase et al. (2023) show that directly editing localized weights is not always the most effective way to alter model behavior. Chen et al. (2024) identify neurons responsible for safety alignment in LLMs.

Our work complements these efforts by demonstrating that capabilities can be localized at the level of attention heads and that ablating these components enables targeted capability removal or modification. We hope that future work can build upon our findings to perform deeper mechanistic studies of capability localization.

2.4. Unlearning and model editing

Our work has some similarities to unlearning and model editing, but our goal fundamentally differs from that of unlearning. Unlearning methods aim to to reliably remove knowledge from a model (Bourtoule et al., 2021; Yan et al., 2022; Xu et al., 2024). Although much of our evaluations involve measuring degradation in task-specific performance, producing an unlearned model is not our goal – we are damaging model performance primarily for the goal of localization.

Additionally, most unlearning work focuses on unlearning specific factual information (parametric knowledge) from a dataset (Guo et al., 2023; Graves et al., 2020; Eldan & Russinovich, 2024). Some work aims to unlearn or edit capabilities, but this approach is less studied and it is often unclear what the definition of capability unlearning should be (Li et al., 2024a).

2.5. Expert specialization

Similar to our findings, mixture-of-experts (MoE) architectures were designed to utilize the benefits of specialization within neural networks by routing inputs to sparse subsets of experts (Shazeer et al., 2017). Prior work has investigated expert specialization and routing strategies, finding that specialization can improve performance and efficiency (Huang et al., 2024; Lo et al., 2025; Guo et al., 2025).

Although MoE models operate on feedforward layers rather than attention heads, they provide evidence that sparse, specialized computation is beneficial. Closer to our setting, Piękos et al. (2025) introduce Mixture of Sparse Attention (MoSA), which routes tokens to a sparse subset of attention heads and achieves improved performance over full attention. These results align with our findings that attention heads naturally specialize and that only a small subset is critical for executing specific capabilities.

3. Problem Setup

Notation We consider a transformer-based large language model M with L layers and H attention heads per layer, for a total of $N = L \times H$ attention heads. We denote an individual attention head as $h_{l,i}$ where $l \in \{1, ..., L\}$ is the layer index and $i \in \{1, ..., H\}$ is the head index within that layer. Each attention head computes an attention-weighted sum of value vectors, producing an output vector that contributes to the residual stream.

Task-specific heads A *task-specific head* for a given task T is an attention head whose removal causes substantial performance degradation on T while minimally impacting performance on other unrelated tasks. *Task* and *capability* are both used to refer to behaviors exhibited by LLMs which do not solely rely on factual knowledge or memorization.

Head Ablation To measure the causal effect of an attention head on model performance, we use a *head ablation* or *knockout* procedure. For a given attention head h, ablation is performed by setting its output to the zero vector: $h.\texttt{attn\_output} \leftarrow \mathbf{0}$.

We evaluate the model's performance on a task of interest T using an evaluation dataset $\mathcal{E}$, measuring accuracy as the fraction of correct responses on $\mathcal{E}$. By comparing the model's baseline accuracy $\text{Acc}_T(M)$ with its accuracy after ablating head h, denoted $\text{Acc}_T(M \setminus \{h\})$, we quantify that head's contribution to performance on T. The performance degradation $\Delta_h T = \text{Acc}_T(M) - \text{Acc}_T(M \setminus \{h\})$ serves as our measure of head importance.

Problem Statement Given a language model M and a task T represented by an evaluation dataset $\mathcal{E}$, our goal is to identify the set of task-specific heads $H_T \subset \{h_{1,1}, ..., h_{L,H}\}$ that are most critical for performance on T. Specifically, we aim to find the k heads whose ablation causes the largest performance degradation on T.

4. Method

Our findings establish the existence of task-specific attention heads in large language models. While this phenomenon reveals a structured organization of model capabilities, it

Algorithm 1 Compressed Sensing Head Identification

Input: LLM M, evaluation data $\mathcal{E}$, measurements M_{evals}, target count k
Parameter: Matrix Construction Strategy $\mathcal{S}$ (Bernoulli or Stratified)
Output: Task-specific heads H
$\Phi \leftarrow \text{ConstructMatrix}(N, M_{evals}, \mathcal{S})$
Initialize observation vector $y \in \mathbb{R}^{M_{evals}}$
for $i = 1$ to M_{evals} **do**
  Configure model: for each head j, ablate if $\Phi_{ij} = 1$
  $y_i \leftarrow \text{Evaluate}(M, \mathcal{E})$
end for
$\hat{x} \leftarrow \text{Lasso}(\Phi, y)$
$H \leftarrow$ Indices of the k smallest coefficients in $\hat{x}$
Return H

also raises the question of how such heads can be identified in practice. To this end, we present an compressed sensing based algorithm which identifies task-specific heads based on their contributions to task performance. The method is able to identify these heads efficiently by exploiting their extreme sparsity and additivity.

Naive approach We first consider a naive approach to finding task-specific heads in a greedy manner. One by one, ablate each head and record the accuracy of the resulting model on the task of interest. Select the head that led to the largest performance degradation and add it to a set of task-specific heads. Then repeat the comprehensive ablation strategy k times until k task-specific heads have been obtained. This procedure involves $N \times k$ evaluations of the model. We can slightly improve efficiency by simply performing one set of N evaluations and taking the top k heads (ie. *one-shot greedy*). Both of these greedy variants work to identify task specific heads (see Table 4), but they are extremely inefficient, motivating development of our compressed sensing approach.

4.1. Compressed Sensing

While greedy approaches provide a reliable baseline for identifying task-specific heads, they scale linearly with the total number of attention heads N. Given that modern large language models contain thousands of heads, a $\Theta(N)$ search complexity becomes computationally prohibitive. To address this, we leverage techniques from Compressed Sensing to identify task-specific heads with significantly greater efficiency.

The method relies on two key premises. The first is the *sparsity assumption*: for any given task, only a small subset k of the total N heads ($k \ll N$) significantly contributes to model performance. The second is the *additivity assumption*: we posit that for the purpose of ablation, the aggregate effect of removing multiple heads is approximately the sum of their individual marginal contributions. While neural networks are inherently non-linear, we assume that locally—relative to the model's baseline performance—the interactions between heads are dominated by their first-order additive effects.

Under these assumptions of sparsity and approximate linearity, theory from Compressed Sensing suggests that the critical heads can be recovered from a small number of measurements M, where $M \ll N$. Specifically, for sparse linear signals, recovery is possible with $M \approx O(k \log(N/k))$ measurements. This efficiency of recovery informally motivates our approach, offering the possibility of a substantial reduction in computational cost compared to the linear scaling of greedy methods.

We formalize the head identification problem as a linear system $y = \Phi x + \epsilon$. Here, $x \in \mathbb{R}^N$ represents the latent impact vector of ablating each attention head. $\Phi \in \{0,1\}^{M \times N}$ is the binary *measurement matrix*, where each row represents a specific ablation configuration. We define an entry $\Phi_{ij} = 1$ to indicate that head j is **ablated** in the i-th evaluation, while $\Phi_{ij} = 0$ indicates the head remains active. The vector $y \in \mathbb{R}^M$ contains the observed model performance for each configuration.

By modeling the ablation response as this linear system, we effectively treat higher-order interactions between heads as noise (ϵ). The validity of this linear approximation is shown by our empirical results, which demonstrate that this formulation reliably finds task-specific heads.

To recover the impact vector x, we solve the following Lasso optimization problem, which uses L_1 regularization to enforce sparsity:

$$\hat{x} = \arg\min_x \frac{1}{2M} \|y - (\beta_0 + \Phi x)\|_2^2 + \lambda \|x\|_1 \tag{1}$$

where β_0 represents the baseline performance. In this formulation, the coefficient $\hat{x}_j$ captures the change in performance caused by ablating head j. Consequently, a large *negative* coefficient implies that ablating head j causes a significant drop in performance. We therefore identify the task-specific heads by selecting the indices corresponding to the smallest (most negative) coefficients in $\hat{x}$.

Measurement Matrix Construction The efficiency and accuracy of recovery depend critically on the design of the measurement matrix Φ. We propose two construction strategies:

1. **Bernoulli Sampling (Random):** We construct Φ by sampling each entry i.i.d. from a Bernoulli distribution. This corresponds to the standard compressed sensing approach where each head is independently ablated

with a fixed probability. While theoretically sound, purely random sampling may yield columns with high variance in their support (i.e., some heads are ablated significantly more often than others purely by chance).

2. **Stratified Sampling (Balanced):** To mitigate the variance of random sampling, we enforce a balancing constraint on the columns of Φ. We construct the matrix such that $\sum_{i=1}^{M} \Phi_{ij} \approx C$ for all heads j. This ensures that every head is "measured" (ablated) in an approximately equal number of evaluations, stabilizing the regression estimates.

Empirically, we find that the Stratified approach offers superior stability. Both variants allow us to recover the true set of k task-specific heads with high fidelity using only a fraction of the evaluations required by greedy search.

The complete procedure is formalized in Algorithm 1.

5. Experiments

5.1. Evaluation setup

We evaluate our task-specific head identification procedure across multiple dimensions:

Task-specific degradation: We measure performance degradation on the task of interest after ablating the identified heads. Effective task-specific heads should cause substantial drops in task performance.

Specificity: We measure performance on unrelated tasks to ensure that ablating task-specific heads does not broadly impair the model. We expect minimal degradation on general language capability benchmarks.

Generalization: When available, we evaluate some capabilities on multiple datasets. Knocking out task-specific heads should impact performance regardless of the dataset used to evaluate the particular capability.

5.2. Implementation Details

Datasets We consider four main capabilities: mathematical reasoning, code generation, swearing/profanity generation, and rhyming ability. We evaluate math capabilities via the GSM8K (Cobbe et al., 2021) and Arithmetic (Brown et al., 2020) datasets, code generation via MBPP (Austin et al., 2021) and HumanEval (Chen et al., 2021), and swearing and rhyming via custom datasets.

We use subsets of these datasets in our method for head identification. We use 100-sample subsets of GSM8K and MBPP to identify math and coding heads, respectively, and we use a subset of our custom swearing and rhyming prompts to identify the corresponding heads.

We evaluate both on task-specific datasets and on a suite of general capability benchmarks including HellaSwag (Zellers et al., 2019), BoolQ (Clark et al., 2019a), Arc Challenge (Clark et al., 2018), and MMLU (Hendrycks et al., 2021). All final evaluation results are reported on full datasets rather than the subsets used for efficient identification. See Appendix A for additional details on hyperparameters, implementation, and custom datasets.

Models We analyze five models, three from the Llama family (Llama 3.1 8B, Llama 3.2 3B, and Llama 3.2 1B) and two from the Qwen family (Qwen 2.5 3B and Qwen 2.5 3B), all instruction finetuned (Grattafiori et al., 2024; Qwen et al., 2025). Details of the models are shown in Table 1.

Table 1. Number of layers, heads per layer, and total heads in each of the models used in our experiments.

MODEL	LAYERS L	HEADS H	TOTAL HEADS N
LLAMA-3.1-8B	32	32	1024
LLAMA-3.2-3B	28	24	672
LLAMA-3.2-1B	16	32	512
QWEN-2.5-7B	28	28	784
QWEN-2.5-3B	32	16	512

Task-specific head identification Our Stratified Compressed Sensing approach reliably identifies task-specific attention heads across a range of capabilities, including mathematical reasoning, code generation, and linguistic behaviors such as swearing and rhyming. Across five model variants, ablating the top five identified heads produces substantial degradations in task-specific performance while leaving general language abilities largely intact. Table 2 summarizes these results. Although the magnitude of localization varies by task and model scale, the overall pattern is consistent: task-relevant heads can be removed with minimal collateral impact on unrelated benchmarks.

We identify a small set of *universal heads* in some models that impact several tasks simultaneously (see Section 6.1). Although these heads are sometimes returned by our method, we filter them out to focus on task-specific localization.

Capability generalization Task-specific heads are not tied to individual datasets, but instead generalize across evaluations that measure the same underlying capability. As shown in Table 3, heads identified using GSM8K substantially degrade performance on Arithmetic, and vice versa. Similarly, heads identified on MBPP also impact HumanEval. Notably, two of the top five heads identified for GSM8K are also identified when using Arithmetic, indicating that both datasets elicit the same underlying mathematical mechanisms. See Appendix D for a complete list of identified task-specific heads.

Table 2. Ablating task-specific heads identified by compressed sensing drastically reduces task-specific performance while leaving general language performance relatively unaffected. Top five task-specific heads are ablated in Llama3.1-8B. Δ Task indicates the change in task-specific performance of the ablated model relative to a non-ablated baseline. Δ Gen indicates the change in general language abilities via an average of accuracies on HellaSwag, BoolQ, Arc Challenge, and MMLU.

MODEL	TASK	Δ TASK ↓	Δ GEN ↑
MATH			
LLAMA-3.1-8B	GSM8K	−48.4	−1.1
LLAMA-3.2-3B	GSM8K	−41.7	−2.3
LLAMA-3.2-1B	GSM8K	−23.0	−2.9
QWEN-2.5-7B	GSM8K	−65.4	−1.8
QWEN-2.5-3B	GSM8K	−32.3	−0.5
CODE			
LLAMA-3.1-8B	MBPP	−16.0	−2.0
LLAMA-3.2-3B	MBPP	−11.0	−0.7
LLAMA-3.2-1B	MBPP	−6.2	−1.2
QWEN-2.5-7B	MBPP	−36.8	−3.6
QWEN-2.5-3B	MBPP	−53.6	−2.2
LANGUAGE			
LLAMA-3.1-8B	SWEAR	−85.4	−0.4
	RHYME	−34.5	−2.8
LLAMA-3.2-3B	SWEAR	−48.4	−1.0
	RHYME	−15.9	−0.3
LLAMA-3.2-1B	SWEAR	−98.2	−1.8
	RHYME	−41.6	−1.4
QWEN-2.5-7B	SWEAR	−60.4	−0.1
	RHYME	−38.9	−6.2
QWEN-2.5-3B	SWEAR	−24.1	−0.9
	RHYME	−15.9	−0.5

Table 3. Heads identified on one datasets also impact performance on other datasets that evaluate the same task. Δ Task indicates change in performance on that dataset and Δ Gen indicates change in performance across an average of general ability benchmarks (HellaSwag, BoolQ, Arc Challenge, and MMLU).

ID ON	EVAL ON	Δ TASK ↓	Δ GEN ↑
MATH			
GSM8K	GSM8K	−48.4	−1.1
	ARITH	−64.4	−1.1
ARITH	GSM8K	−37.5	−0.4
	ARITH	−70.1	−0.4
CODING			
MBPP	MBPP	−16.0	−2.0
	HEVAL	−18.3	−2.0

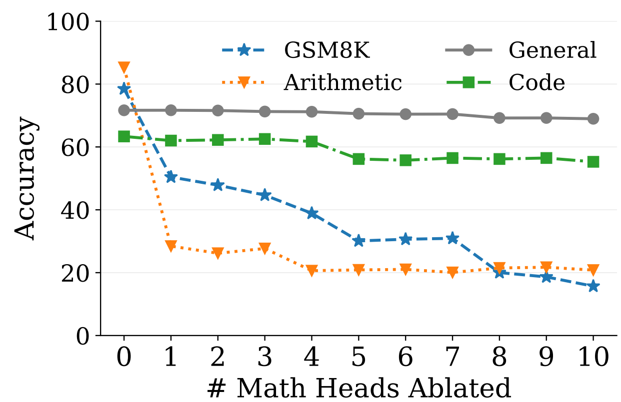

Figure 2. Ablating increasing numbers of top math heads degrades GSM8K and Arithmetic performance while leaving general language abilities (average of HellaSwag, BoolQ, Arc Challenge, and MMLU) unaffected. We begin to see diminishing returns on task-specific degradation as we continue ablating additional heads.

Head identification methods We compare greedy baselines with our compressed sensing methods in Table 4. Stratified Compressed Sensing (balanced measurement matrix) consistently matches or exceeds standard compressed sensing (Bernoulli measurement matrix) in terms of task-specific degradation, while requiring far fewer evaluations.

Sparsity of task-specific heads For our main analyses, we focus on the top five task-specific heads. This choice is motivated by a clear plateauing effect: beyond the first few heads, ablating additional heads yields diminishing returns in task-specific degradation. Figure 2 illustrates this behavior for mathematical reasoning. Ablating the first head accounts for a large fraction of the performance drop on GSM8K and Arithmetic, while further ablations provide progressively smaller additional degradation. This behavior further supports our assumption of extreme sparsity, where only a small number of heads contribute meaningfully to a given capability.

6. Discussion

We find that capability localization manifests to varying degrees across both tasks and model scales. Across five models, our results consistently demonstrate strong localization for four distinct capabilities. Importantly, our method does not explicitly search for heads that affect only a single task, nor does it rely on contrastive objectives. Nevertheless, the heads it identifies are typically highly specific: ablating them substantially degrades performance on the target task while leaving other capabilities largely intact. This pattern suggests that Transformer models naturally organize some task-relevant computation into specialized attention heads,

Table 4. Comparison between greedy, one shot greedy (1S-Greedy), compressed sensing with Bernoulli measurement matrix (CS_B), and compressed sensing with Stratified sampling measurement matrix (CS_S). Change in task-specific performance, general performance (average of HellaSwag, BoolQ, Arc Challenge, and MMLU accuracies), and number of evaluations required are reported.

TASK	METHOD	Δ TASK↓	Δ GEN↑	# EVALS↓
		MATH		
GSM8K	GREEDY	−55.4	−1.3	5120
	1S-GREEDY	−47.9	−2.4	1024
	CS_B	−39.5	−1.9	200
	CS_S	−48.4	−1.1	100
		CODE		
MBPP	GREEDY	−20.0	−0.3	5120
	1S-GREEDY	−17.0	−2.0	1024
	CS_B	−9.4	−0.6	200
	CS_S	−16.0	−2.0	200
		LANGUAGE		
SWEAR	GREEDY	−87.5	−0.8	5120
	1S-GREEDY	−59.9	−0.8	1024
	CS_B	−85.4	−0.5	400
	CS_S	−85.4	−0.4	200
RHYME	GREEDY	−59.3	−2.7	5120
	1S-GREEDY	−43.4	−2.5	1024
	CS_B	−28.3	−2.5	100
	CS_S	−34.5	−2.8	100

rather than distributing it uniformly across the network.

Our results further indicate a relationship between model scale and the degree of capability localization. Larger models exhibit stronger localization: ablating the top five task-specific heads leads to substantially larger degradations in target-task performance compared to smaller models. One plausible explanation is that increased model capacity provides greater flexibility for specialization, allowing individual attention heads to assume more focused functional roles rather than sharing responsibility across tasks.

All of the models we study utilize Grouped Query Attention (GQA) (Ainslie et al., 2023), and we sometimes find that multiple task-specific heads are within the same group (see complete lists of task-specific heads in Table 9, eg. Arithmetic heads on Llama 3.2 3B, GSM8k heads on both Qwen models). In GQA, heads within a group share key and value projections while differing only in their query projections. This clustering suggests that task-specific capabilities may rely on a shared key–value subspace that is accessed by multiple heads in parallel.

Despite finding clear and consistent evidence of strong localization of four capabilities, we also discovered other types of interesting behavior. These additional phenomena indicate that task-specific localization does not necessarily explain the behavior of all heads within a model and opens up directions for future study into how head localization tends to emerge in the ways we have observed.

Table 5. Ablating universal heads leads to performance degradation across multiple tasks. Δ Math indicates the change in average performance across GSM8K and Arithmetic; Δ Code indicates the same for MBPP and HumanEval; Δ Lang for Swearing and Rhyming; and Δ Gen for HellaSwag, BoolQ, Arc C, and MMLU.

	Δ MATH↓	Δ CODE↓	Δ LANG↓	Δ GEN↓
		LLAMA-3.1-8B		
L0H31	−5.8	−47.0	−6.7	−13.2
L1H29	−81.3	−63.4	+0.3	−37.9
L1H31	−81.2	−40.9	−8.0	−25.8
		LLAMA-3.2-3B		
L0H22	−27.3	−18.0	+1.0	−12.8
L0H23	−4.1	−19.2	−9.8	−14.2
L1H23	−66.1	−48.7	−3.8	−32.6
		LLAMA-3.2-1B		
L0H29	−10.2	−24.2	+7.5	−9.3
L0H31	−16.4	−22.5	−16.4	−4.1
L1H29	−41.4	−31.6	−8.4	−23.4
L1H31	−41.8	−31.6	−2.2	−23.8

6.1. Universal Heads

In addition to task-specific heads, we identify a small set of *universal heads*. These heads are consistently elicited across different tasks, and we therefore filter them out from task-specific analyses and study them separately. As shown in Table 5, universal heads appear across all Llama models and are localized to similar positions, typically in the first or second layer and among the final heads within those layers. Ablating these heads causes broad performance degradation across diverse tasks, including both task-specific and general language benchmarks.

Unlike task-specific heads, universal heads induce qualitatively different failure modes. Rather than simply producing incorrect answers, ablating these heads often leads to pathological behaviors such as repetitive or degenerate outputs. When ablating L1H29 in Llama 3.1 8B, the model outputs extremely low likelihood for all choices on questions from multiple choice datasets (Arithmetic, HellaSwag, BoolQ, Arc Challenge, MMLU). On GSM8k, the model often repeats one sentence from its reasoning trace; on MBPP, the model consistently returns the same function to determine if a number is prime regardless of the question; and on HumanEval, the model outputs repeated backticks (‘). These behaviors suggest that universal heads support core functionality required for coherent question answering and language generation, rather than specialized task execution.

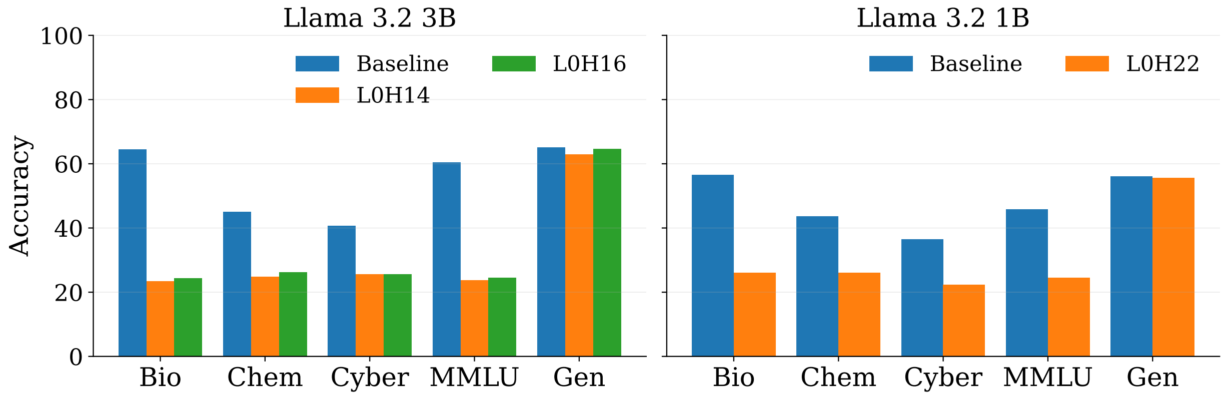

Figure 3. Knowledge-based multiple choice heads identified in Llama 3.2 3B and Llama 3.2 1B impact all WMDP subtypes as well as MMLU. Ablating just one of these heads reduces performance on WMDP and MMLU to random chance (approximately 25%) while leaving general performance (average across HellaSwag, BoolQ, and Arc C) unaffected.

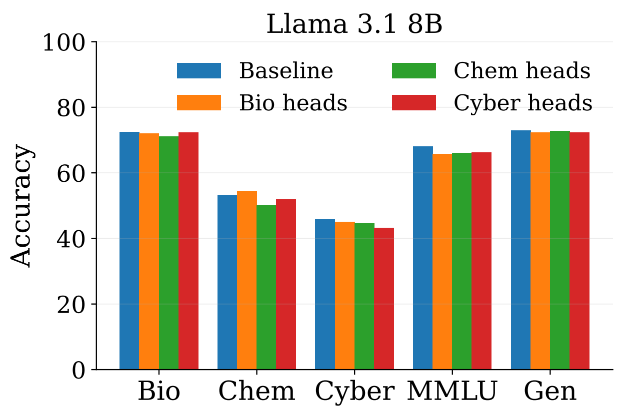

Figure 4. WMDP subtasks have very weak localization in Llama 3.1 8B.

6.2. Scale dependence of localization

A scale-dependent pattern emerges in how certain task-specific capabilities localize to attention heads. We apply our localization method to WMDP, a benchmark that measures hazardous knowledge across biology, chemistry, and cybersecurity (Li et al., 2024b). We find evidence of weak localization in Llama 3.1 8B but there is overlap between subtasks and we are unable to obtain large performance degradations using any method, as shown in Figure 4.

However, as seen in Figure 3, we find that at smaller model scales (Llama 3.2 3B and Llama 3.2 1B) a qualitatively different structure emerges. After filtering out universal heads, we find that all three WMDP subgroups share one or two dominant heads whose ablation accounts for most of the performance degradation. Ablating these shared heads also severely degrades performance on MMLU, a behavior not observed for any WMDP-specific heads in Llama 3.1 8B. This suggests that, at smaller scales, performance on these datasets may be predominantly mediated by shared "knowledge-based multiple-choice" heads rather than task-specific mechanisms. Ablating one of these heads reduces both WMDP and MMLU performance to near random chance but preserves general language performance. We find no evidence of analogous knowledge-based multiple-choice heads in Llama 3.1 8B.

Given that MMLU and WMDP share a very similar structure, it appears that format-specific, rather than task-specific heads may emerge at smaller scales. Together, these results indicate that task-specific heads for specific knowledge such as in the WMDP benchmark may emerge only at larger scales, while smaller models could rely on shared, format-level mechanisms that support reasoning across tasks.

7. Conclusion

Our findings demonstrate that several high-level capabilities in LLMs are highly localized to small sets of attention heads. Across five models, we identify task-specific heads for four capabilities (mathematical reasoning, code generation, swearing, and rhyming) whose ablation substantially degrades performance on the corresponding task while largely preserving performance on unrelated tasks. We introduce an efficient, inference-only compressed-sensing–based method for identifying such heads, enabling reliable recovery with a small number of model evaluations. In addition, we find evidence for universal heads that contribute broadly across tasks, as well as scale-dependent patterns in how capabilities are localized. Together, these results provide insight into the functional organization of Transformer models and suggest new avenues for research into interpretability, model editing, and AI safety.

References

Ainslie, J., Lee-Thorp, J., De Jong, M., Zemlyanskiy, Y., Lebrón, F., and Sanghai, S. Gqa: Training generalized multi-query transformer models from multi-head checkpoints. *arXiv preprint arXiv:2305.13245*, 2023.

Austin, J., Odena, A., Nye, M., Bosma, M., Michalewski, H., Dohan, D., Jiang, E., Cai, C., Terry, M., Le, Q., and Sutton, C. Program synthesis with large language models, 2021. URL https://arxiv.org/abs/2108.07732.

Bourtoule, L., Chandrasekaran, V., Choquette-Choo, C. A., Jia, H., Travers, A., Zhang, B., Lie, D., and Papernot, N. Machine unlearning. In *2021 IEEE symposium on security and privacy (SP)*, pp. 141–159. IEEE, 2021.

Bricken, T., Templeton, A., Batson, J., Chen, B., Jermyn, A., Conerly, T., Turner, N., Anil, C., Denison, C., Askell, A., Lasenby, R., Wu, Y., Kravec, S., Schiefer, N., Maxwell, T., Joseph, N., Hatfield-Dodds, Z., Tamkin, A., Nguyen, K., McLean, B., Burke, J. E., Hume, T., Carter, S., Henighan, T., and Olah, C. Towards monosemanticity: Decomposing language models with dictionary learning. *Transformer Circuits Thread*, 2023. https://transformer-circuits.pub/2023/monosemantic-features/index.html.

Brown, T. B., Mann, B., Ryder, N., Subbiah, M., Kaplan, J., Dhariwal, P., Neelakantan, A., Shyam, P., Sastry, G., Askell, A., Agarwal, S., Herbert-Voss, A., Krueger, G., Henighan, T., Child, R., Ramesh, A., Ziegler, D. M., Wu, J., Winter, C., Hesse, C., Chen, M., Sigler, E., Litwin, M., Gray, S., Chess, B., Clark, J., Berner, C., McCandlish, S., Radford, A., Sutskever, I., and Amodei, D. Language models are few-shot learners. 2020.

Candes, E. and Wakin, M. Wakin, m.b.: An introduction to compressive sampling. ieee signal process. mag. 25(2), 21-30. *Signal Processing Magazine, IEEE*, 25:21 – 30, 04 2008. doi: 10.1109/MSP.2007.914731.

Candes, E. J. and Tao, T. Near-optimal signal recovery from random projections: Universal encoding strategies? *IEEE Transactions on Information Theory*, 52(12):5406–5425, 2006. doi: 10.1109/TIT.2006.885507.

Chen, H., Li, H., Xiao, Z., Gao, L., Zhang, Q., Hu, X., Wang, N., Fu, X., and Zhao, J. Alps: Attention localization and pruning strategy for efficient alignment of large language models, 2025. URL https://arxiv.org/abs/2505.18799.

Chen, J., Wang, X., Yao, Z., Bai, Y., Hou, L., and Li, J. Finding safety neurons in large language models, 2024. URL https://arxiv.org/abs/2406.14144.

Chen, M., Tworek, J., Jun, H., Yuan, Q., de Oliveira Pinto, H. P., Kaplan, J., Edwards, H., Burda, Y., Joseph, N., Brockman, G., Ray, A., Puri, R., Krueger, G., Petrov, M., Khlaaf, H., Sastry, G., Mishkin, P., Chan, B., Gray, S., Ryder, N., Pavlov, M., Power, A., Kaiser, L., Bavarian, M., Winter, C., Tillet, P., Such, F. P., Cummings, D., Plappert, M., Chantzis, F., Barnes, E., Herbert-Voss, A., Guss, W. H., Nichol, A., Paino, A., Tezak, N., Tang, J., Babuschkin, I., Balaji, S., Jain, S., Saunders, W., Hesse, C., Carr, A. N., Leike, J., Achiam, J., Misra, V., Morikawa, E., Radford, A., Knight, M., Brundage, M., Murati, M., Mayer, K., Welinder, P., McGrew, B., Amodei, D., McCandlish, S., Sutskever, I., and Zaremba, W. Evaluating large language models trained on code, 2021. URL https://arxiv.org/abs/2107.03374.

Clark, C., Lee, K., Chang, M.-W., Kwiatkowski, T., Collins, M., and Toutanova, K. Boolq: Exploring the surprising difficulty of natural yes/no questions, 2019a. URL https://arxiv.org/abs/1905.10044.

Clark, K., Khandelwal, U., Levy, O., and Manning, C. D. What does bert look at? an analysis of bert's attention, 2019b. URL https://arxiv.org/abs/1906.04341.

Clark, P., Cowhey, I., Etzioni, O., Khot, T., Sabharwal, A., Schoenick, C., and Tafjord, O. Think you have solved question answering? try arc, the ai2 reasoning challenge, 2018. URL https://arxiv.org/abs/1803.05457.

Cobbe, K., Kosaraju, V., Bavarian, M., Chen, M., Jun, H., Kaiser, L., Plappert, M., Tworek, J., Hilton, J., Nakano, R., Hesse, C., and Schulman, J. Training verifiers to solve math word problems, 2021. URL https://arxiv.org/abs/2110.14168.

Donoho, D. Compressed sensing. *IEEE Transactions on Information Theory*, 52(4):1289–1306, 2006. doi: 10.1109/TIT.2006.871582.

Eldan, R. and Russinovich, M. Who's harry potter? approximate unlearning for LLMs, 2024. URL https://openreview.net/forum?id=PDct7vrcvT.

Elhage, N., Hume, T., Olsson, C., Schiefer, N., Henighan, T., Kravec, S., Hatfield-Dodds, Z., Lasenby, R., Drain, D., Chen, C., Grosse, R., McCandlish, S., Kaplan, J., Amodei, D., Wattenberg, M., and Olah, C. Toy models of superposition. *Transformer Circuits Thread*, 2022. https://transformer-circuits.pub/2022/toy_model/index.html.

Grattafiori, A., Dubey, A., Jauhri, A., Pandey, A., Kadian, A., Al-Dahle, A., Letman, A., Mathur, A., Schelten, A., Vaughan, A., et al. The llama 3 herd of models. *arXiv preprint arXiv:2407.21783*, 2024.

Graves, L., Nagisetty, V., and Ganesh, V. Amnesiac machine learning, 2020. URL https://arxiv.org/abs/2010.10981.

Guo, C., Goldstein, T., Hannun, A., and van der Maaten, L. Certified data removal from machine learning models, 2023. URL https://arxiv.org/abs/1911.03030.

Guo, H., Lu, H., Nan, G., Chu, B., Zhuang, J., Yang, Y., Che, W., Leng, S., Cui, Q., and Jiang, X. Advancing expert specialization for better moe, 2025. URL https://arxiv.org/abs/2505.22323.

Hase, P., Bansal, M., Kim, B., and Ghandeharioun, A. Does localization inform editing? surprising differences in causality-based localization vs. knowledge editing in language models, 2023. URL https://arxiv.org/abs/2301.04213.

Hendrycks, D., Burns, C., Basart, S., Zou, A., Mazeika, M., Song, D., and Steinhardt, J. Measuring massive multitask language understanding, 2021. URL https://arxiv.org/abs/2009.03300.

Huang, Q., An, Z., Zhuang, N., Tao, M., Zhang, C., Jin, Y., Xu, K., Chen, L., Huang, S., and Feng, Y. Harder tasks need more experts: Dynamic routing in moe models. *arXiv preprint arXiv:2403.07652*, 2024.

Jin, Z., Cao, P., Yuan, H., Chen, Y., Xu, J., Li, H., Jiang, X., Liu, K., and Zhao, J. Cutting off the head ends the conflict: A mechanism for interpreting and mitigating knowledge conflicts in language models, 2024. URL https://arxiv.org/abs/2402.18154.

Kim, G., Valentino, M., and Freitas, A. Reasoning circuits in language models: A mechanistic interpretation of syllogistic inference, 2025. URL https://arxiv.org/abs/2408.08590.

Li, M., Davies, X., and Nadeau, M. Circuit breaking: Removing model behaviors with targeted ablation, 2024a. URL https://arxiv.org/abs/2309.05973.

Li, N., Pan, A., Gopal, A., Yue, S., Berrios, D., Gatti, A., Li, J. D., Dombrowski, A.-K., Goel, S., Phan, L., Mukobi, G., Helm-Burger, N., Lababidi, R., Justen, L., Liu, A. B., Chen, M., Barrass, I., Zhang, O., Zhu, X., Tamirisa, R., Bharathi, B., Khoja, A., Zhao, Z., Herbert-Voss, A., Breuer, C. B., Marks, S., Patel, O., Zou, A., Mazeika, M., Wang, Z., Oswal, P., Lin, W., Hunt, A. A., Tienken-Harder, J., Shih, K. Y., Talley, K., Guan, J., Kaplan, R., Steneker, I., Campbell, D., Jokubaitis, B., Levinson, A., Wang, J., Qian, W., Karmakar, K. K., Basart, S., Fitz, S., Levine, M., Kumaraguru, P., Tupakula, U., Varadharajan, V., Wang, R., Shoshitaishvili, Y., Ba, J., Esvelt, K. M., Wang, A., and Hendrycks, D. The wmdp benchmark: Measuring and reducing malicious use with unlearning, 2024b. URL https://arxiv.org/abs/2403.03218.

Lo, K. M., Huang, Z., Qiu, Z., Wang, Z., and Fu, J. A closer look into mixture-of-experts in large language models, 2025. URL https://arxiv.org/abs/2406.18219.

Maini, P., Mozer, M. C., Sedghi, H., Lipton, Z. C., Kolter, J. Z., and Zhang, C. Can neural network memorization be localized?, 2023. URL https://arxiv.org/abs/2307.09542.

McDougall, C., Conmy, A., Rushing, C., McGrath, T., and Nanda, N. Copy suppression: Comprehensively understanding an attention head, 2023. URL https://arxiv.org/abs/2310.04625.

Meng, K., Bau, D., Andonian, A., and Belinkov, Y. Locating and editing factual associations in gpt, 2023. URL https://arxiv.org/abs/2202.05262.

Michel, P., Levy, O., and Neubig, G. Are sixteen heads really better than one?, 2019. URL https://arxiv.org/abs/1905.10650.

Nikankin, Y., Reusch, A., Mueller, A., and Belinkov, Y. Arithmetic without algorithms: Language models solve math with a bag of heuristics. *arXiv preprint arXiv:2410.21272*, 2024.

Olsson, C., Elhage, N., Nanda, N., Joseph, N., DasSarma, N., Henighan, T., Mann, B., Askell, A., Bai, Y., Chen, A., Conerly, T., Drain, D., Ganguli, D., Hatfield-Dodds, Z., Hernandez, D., Johnston, S., Jones, A., Kernion, J., Lovitt, L., Ndousse, K., Amodei, D., Brown, T., Clark, J., Kaplan, J., McCandlish, S., and Olah, C. In-context learning and induction heads, 2022. URL https://arxiv.org/abs/2209.11895.

Panigrahi, A., Saunshi, N., Zhao, H., and Arora, S. Task-specific skill localization in fine-tuned language models. In Krause, A., Brunskill, E., Cho, K., Engelhardt, B., Sabato, S., and Scarlett, J. (eds.), *Proceedings of the 40th International Conference on Machine Learning*, volume 202 of *Proceedings of Machine Learning Research*, pp. 27011–27033. PMLR, 23–29 Jul 2023. URL https://proceedings.mlr.press/v202/panigrahi23a.html.

Piękos, P., Csordás, R., and Schmidhuber, J. Mixture of sparse attention: Content-based learnable sparse attention via expert-choice routing. *arXiv preprint arXiv:2505.00315*, 2025.

Qwen, :, Yang, A., Yang, B., Zhang, B., Hui, B., Zheng, B., Yu, B., Li, C., Liu, D., Huang, F., Wei, H., Lin, H., Yang, J., Tu, J., Zhang, J., Yang, J., Yang, J., Zhou, J., Lin, J., Dang, K., Lu, K., Bao, K., Yang, K., Yu, L., Li, M., Xue, M., Zhang, P., Zhu, Q., Men, R., Lin, R., Li, T., Tang, T., Xia, T., Ren, X., Ren, X., Fan, Y., Su, Y., Zhang, Y., Wan, Y., Liu, Y., Cui, Z., Zhang, Z., and Qiu, Z. Qwen2.5 technical report, 2025. URL https://arxiv.org/abs/2412.15115.

Shazeer, N., Mirhoseini, A., Maziarz, K., Davis, A., Le, Q., Hinton, G., and Dean, J. Outrageously large neural networks: The sparsely-gated mixture-of-experts layer. *arXiv preprint arXiv:1701.06538*, 2017.

Tang, H., Lin, Y., Lin, J., Han, Q., Hong, S., Yao, Y., and Wang, G. Razorattention: Efficient kv cache compression through retrieval heads, 2024. URL https://arxiv.org/abs/2407.15891.

Templeton, A., Conerly, T., Marcus, J., Lindsey, J., Bricken, T., Chen, B., Pearce, A., Citro, C., Ameisen, E., Jones, A., Cunningham, H., Turner, N. L., McDougall, C., MacDiarmid, M., Freeman, C. D., Sumers, T. R., Rees, E., Batson, J., Jermyn, A., Carter, S., Olah, C., and Henighan, T. Scaling monosemanticity: Extracting interpretable features from claude 3 sonnet. *Transformer Circuits Thread*, 2024. URL https://transformer-circuits.pub/2024/scaling-monosemanticity/index.html.

Voita, E., Talbot, D., Moiseev, F., Sennrich, R., and Titov, I. Analyzing multi-head self-attention: Specialized heads do the heavy lifting, the rest can be pruned, 2019. URL https://arxiv.org/abs/1905.09418.

Wang, X., Wang, L., Lin, B., and Zhang, Y. Headmap: Locating and enhancing knowledge circuits in LLMs. In *The Thirteenth International Conference on Learning Representations*, 2025. URL https://openreview.net/forum?id=jUsrbOuQ5e.

Wu, W., Wang, Y., Xiao, G., Peng, H., and Fu, Y. Retrieval head mechanistically explains long-context factuality, 2024. URL https://arxiv.org/abs/2404.15574.

Xiao, G., Tang, J., Zuo, J., Guo, J., Yang, S., Tang, H., Fu, Y., and Han, S. Duoattention: Efficient long-context llm inference with retrieval and streaming heads, 2024. URL https://arxiv.org/abs/2410.10819.

Xu, J., Wu, Z., Wang, C., and Jia, X. Machine unlearning: Solutions and challenges. *IEEE Transactions on Emerging Topics in Computational Intelligence*, 8 (3):2150–2168, June 2024. ISSN 2471-285X. doi: 10.1109/tetci.2024.3379240. URL http://dx.doi.org/10.1109/TETCI.2024.3379240.

Yan, H., Li, X., Guo, Z., Li, H., Li, F., and Lin, X. Arcane: An efficient architecture for exact machine unlearning. In Raedt, L. D. (ed.), *Proceedings of the Thirty-First International Joint Conference on Artificial Intelligence, IJCAI-22*, pp. 4006–4013. International Joint Conferences on Artificial Intelligence Organization, 7 2022. doi: 10.24963/ijcai.2022/556. URL https://doi.org/10.24963/ijcai.2022/556. Main Track.

Yin, K. and Steinhardt, J. Which attention heads matter for in-context learning? *arXiv preprint arXiv:2502.14010*, 2025.

Yuan, H., Cao, P., Jin, Z., Chen, Y., Zeng, D., Liu, K., and Zhao, J. Whispers that shake foundations: Analyzing and mitigating false premise hallucinations in large language models, 2024. URL https://arxiv.org/abs/2402.19103.

Zellers, R., Holtzman, A., Bisk, Y., Farhadi, A., and Choi, Y. Hellaswag: Can a machine really finish your sentence?, 2019. URL https://arxiv.org/abs/1905.07830.

Zhang, W., Wan, C., Zhang, Y., ming Cheung, Y., Tian, X., Shen, X., and Ye, J. Interpreting and improving large language models in arithmetic calculation, 2024. URL https://arxiv.org/abs/2409.01659.

Zheng, Z., Wang, Y., Huang, Y., Song, S., Yang, M., Tang, B., Xiong, F., and Li, Z. Attention heads of large language models: A survey. *arXiv preprint arXiv:2409.03752*, 2024.

Zhou, Z., Yu, H., Zhang, X., Xu, R., Huang, F., Wang, K., Liu, Y., Fang, J., and Li, Y. On the role of attention heads in large language model safety, 2025. URL https://arxiv.org/abs/2410.13708.

A. Implementation Details

The methods require repeated evaluation of model performance on a task of interest. To maintain computational efficiency during the head identification phase, we do not use complete datasets. Instead, we sample a representative subset of each evaluation dataset, which we empirically determined to be sufficient for robust identification of task-specific heads. Through preliminary experiments varying the sample size, we found that 100 samples provides stable head rankings while minimizing evaluation time. Once task-specific heads are identified using these subsets, we validate our results by evaluating the model with ablated heads on the full test datasets.

A.1. Hyperparameter Search

The compressed sensing method development involved a hyperparameter search to identify the best number of masks and sparsity. If the sparsity is too high and too many heads are ablated, the model performance will be harmed too much and task-specific heads will not be able to be recovered. If the number of masks is too high, we do not gain as much efficiency savings. We want to balance both hyperparameters to essentially get just enough coverage to have sufficient signal for identifying the task-specific heads. Based on minimal necessary coverage, we use at least 100 masks and 0.01 sparsity. We increase masks up to 400 and experiment with sparsities up to 0.1.

We run each hyperparameter setting using 100 samples from the target dataset, which returns a set of heads. We ablate the top heads and evaluate the performance on the task of interests (still using the reduced 100-sample dataset). We select the hyperparameters that generate the heads that lead to the largest performance degradation upon ablation. Once hyperparameters are fixed, we evaluate using full datasets.

A.2. Custom tasks

Swearing We generate 12 prompts designed to elicit generation of swear words in LLMs. We then compare generated words with a profanity dataset[1] to determine the number of profanities generated. Performance on ablated models is determined by computing the drop in number of generated words relative to the unablated baseline.

Rhyming We design a set of rhyming words that includes both easy and challenging rhymes. We do this through a combination of manual and AI-assisted curation. We use the CMU Pronouncing Dictionary[2] to aid with automated rhyme recognition.

B. Additional Results

Here we include full sets of results that were summarized in the main paper. Table 6 shows the performance degradation on Llama 3.1 8B for varying numbers of top k heads ablated. Table 7 includes the per-task performance degradation when each identified universal head is ablated.

C. WMDP and Knowledge-based Multiple Choice Heads

We include the full set of results for knowledge-based multiple choice heads identified in Llama 3.2 3B and Llama 3.2 1B in Table 8. Evaluations are grouped based on whether or not they are knowledge-based multiple choice tasks and impacted by the task-specific head ablation.

D. Task-specific heads

Table 9 and Table 10 includes the heads identified by each method, across models and tasks.

[1] `https://huggingface.co/datasets/mmathys/profanity`
[2] `http://www.speech.cs.cmu.edu/cgi-bin/cmudict`

Table 6. Effects of ablating different numbers of task-specific heads on task accuracy and generalization.

TASK	# HEADS	ACC	Δ TASK	Δ GEN
		MATH		
GSM8K	BL	78.5	–	–
	1	50.4	−28.1	0.0
	2	47.8	−30.7	−0.1
	3	44.7	−33.8	−0.4
	4	38.9	−39.6	−0.5
	5	30.1	−48.4	−1.1
		CODE		
MBPP	BL	58.4	–	–
	1	57.0	−1.4	−0.1
	2	49.8	−8.6	−1.9
	3	44.4	−14.0	−1.9
	4	43.0	−15.4	−2.0
	5	42.4	−16.0	−2.0
		WMDP		
BIO	BL	72.5	–	–
	1	72.5	0.0	−0.2
	2	72.4	−0.1	−0.5
	3	72.4	−0.1	−0.5
	4	72.5	0.0	−1.1
	5	72.0	−0.5	−1.0
CHEM	BL	53.2	–	–
	1	54.7	1.5	0.0
	2	49.8	−3.4	−0.6
	3	49.8	−3.4	−0.7
	4	49.5	−3.7	−0.7
	5	50.0	−3.2	−0.6
CYBER	BL	45.9	–	–
	1	43.7	−2.1	−0.9
	2	43.7	−2.1	−0.8
	3	43.9	−1.9	−0.7
	4	43.8	−2.1	−0.9
	5	43.3	−2.6	−0.9
		LANGUAGE		
SWEAR	BL	100.0	–	–
	1	18.2	−81.8	−0.2
	2	25.0	−75.0	−0.1
	3	9.9	−90.1	−0.1
	4	4.7	−95.3	−0.1
	5	14.6	−85.4	−0.4
RHYME	BL	65.5	–	–
	1	46.9	−18.6	−0.2
	2	37.2	−28.3	−0.5
	3	33.6	−31.9	−0.5
	4	28.3	−37.2	−1.1
	5	31.0	−34.5	−1.0

Table 7. Effect of universal heads.

HEAD	GSM	AR	MBPP	HE	HS	BQ	ARC C	MMLU	W-B	W-CH	W-CY	SWEAR	RHYME	**AVG**
							LLAMA-3.1-8B							
BL	78.5	85.3	58.4	68.3	79.3	84.1	55.2	68.0	72.5	53.2	45.9	100.0	65.5	70.3
L0H31	−9.1	−2.6	−25.6	−68.3	−32.4	−12.4	−3.5	−4.4	−1.5	−2.5	−1.7	−12.5	−0.9	−13.6
L1H29	−77.3	−85.3	−58.4	−68.3	−49.3	−25.2	−32.4	−44.8	−47.4	−29.7	−18.3	−0.25	+0.8	−41.2
L1H31	−77.2	−85.3	−13.6	−68.3	−47.8	−22.3	−32.8	−0.2	+0.1	−0.4	+0.3	−16.7	+0.8	−28.0
							LLAMA-3.2-3B							
BL	65.7	68.3	46.2	51.2	70.5	78.4	46.4	60.4	64.5	45.1	40.7	100.0	67.3	61.9
L0H22	−22.1	−32.5	−15.8	−20.1	−23.4	−13.8	−6.9	−6.9	−3.8	−2.5	−3.5	+1.1	+0.9	−11.5
L0H23	−2.9	−5.3	−34.8	−3.7	−37.6	−17.1	−1.7	−0.3	−0.6	−1.0	−1.3	−18.7	−0.9	−9.7
L1H23	−64.4	−67.8	−46.2	−51.2	−42.3	−30.8	−21.7	−35.6	−41.0	−22.3	−15.2	−6.6	−0.9	−34.3
							LLAMA-3.2-1B							
BL	32.9	51.7	32.2	31.1	60.7	69.5	38.1	45.9	56.5	43.6	36.4	100.0	41.6	50.2
L0H29	−19.2	−1.1	−17.4	−31.1	−16.4	−10.0	−2.9	−7.9	−8.1	−8.1	−3.7	+15.9	−0.9	−8.5
L0H31	−17.9	−14.9	−32.2	−12.8	−6.4	−4.1	−6.1	+0.4	+0.6	−0.7	+0.3	−32.7	−0.0	−9.7
L1H29	−31.2	−51.5	−32.2	−31.1	−31.2	−26.2	−15.2	−21.2	−31.1	−16.6	−11.7	−17.7	+0.9	−24.3
L1H31	−31.8	−51.7	−32.2	−31.1	−31.4	−27.4	−14.4	−21.8	−31.9	−17.4	−10.7	−5.3	+0.9	−23.6

Table 8. Single-head performance across tasks. Knowledge-based multiple-choice tasks (Knowledge MC) are grouped separately from non-multiple-choice tasks.

	KNOWLEDGE MC					**NOT KNOWLEDGE MC**									
HEAD	MMLU	W-B	W-CH	W-CY	**AVG**	GSM	AR	MBPP	HE	HS	BOOLQ	ARC C	SWEAR	RHYME	**AVG**
							LLAMA-3.2-3B								
BL	60.4	64.5	45.1	40.7	52.7	65.7	68.3	46.2	51.2	70.5	78.4	46.4	100.0	67.3	66.0
L0H14	−36.7	−41.1	−20.3	−15.1	−28.3	−1.3	+2.2	−0.8	−0.6	−1.5	−5.4	+0.4	+39.8	−0.9	+3.5
L0H16	−35.9	−40.1	−18.9	−15.1	−27.5	+0.3	−0.2	−2.2	−1.2	+0.1	−1.8	+0.4	+20.0	0.0	+1.7
							LLAMA-3.2-1B								
BL	45.9	56.5	43.6	36.4	45.6	32.9	51.7	32.2	31.1	60.7	69.5	38.1	100.0	41.6	50.9
L0H22	−21.3	−30.5	−17.6	−14.0	−20.8	+1.1	−0.6	−0.8	−1.2	+0.3	−1.5	−0.1	−14.8	+1.8	−1.8

Table 9. Task-specific heads identified in Llama 3.1 8B on various tasks, using various methods.

TASK	METHOD	TOP 5 HEADS
		MATH
GSM8K	GREEDY	L16H21, L15H13, L18H18, L18H31, L0H28
GSM8K	1S-GREEDY	L16H21, L15H13, L13H18, L1H30, L0H28
GSM8K	CS_B	L15H13, L16H21, L13H18, L30H3, L9H19
GSM8K	CS_S	L15H13, L16H2, L12H12, L16H21, L13H18
ARITH	GREEDY	L15H13, L16H21, L18H18, L7H27, L31H14
ARITH	1S-GREEDY	L15H13, L16H21, L14H0, L31H14, L13H7
ARITH	CS_S	L15H13, L16H21, L11H16, L13H16, L21H27
		CODE
MBPP	GREEDY	L24H31, L18H7, L7H6, L26H16, L24H14
MBPP	1S-GREEDY	L24H31, L6H19, L1H28, L12H30, L4H11
MBPP	CS_B	L4H13, L10H17, L24H31, L30H6, L8H16
MBPP	CS_S	L15H24, L1H28, L24H31, L31H24, L31H25
		LANGUAGE
SWEAR	GREEDY	L11H2, L1H17, L1H5, L0H13, L19H21
SWEAR	1S-GREEDY	L11H2, L9H10, L5H17, L10H18, L14H14
SWEAR	CS_B	L11H2, L23H24, L11H18, L11H15, L31H22
SWEAR	CS_S	L11H2, L26H7, L14H12, L1H1, L8H15
RHYME	GREEDY	L0H29, L18H4, L0H28, L18H5, L13H28
RHYME	1S-GREEDY	L0H29, L18H5, L28H25, L16H19, L10H22
RHYME	CS_B	L0H29, L29H27, L28H8, L29H0, L30H15
RHYME	CS_S	L0H29, L9H10, L20H1, L14H12, L23H4
		WMDP
BIO	GREEDY	L3H22, L10H3, L11H13, L31H14, L1H5
BIO	1S-GREEDY	L4H16, L3H22, L31H14, L1H24, L6H24
BIO	CS_B	L13H5, L25H18, L31H14, L12H6, L23H13
BIO	CS_S	L10H26, L12H22, L9H9, L21H26, L29H2
CHEM	GREEDY	L0H3, L8H8, L5H3, L10H23, L9H21
CHEM	1S-GREEDY	L0H3, L7H7, L12H4, L2H22, L16H22
CHEM	CS_B	L19H31, L13H18, L9H29, L22H23, L16H22
CHEM	CS_S	L0H24, L0H3, L20H14, L7H21, L18H30
CYBER	GREEDY	L31H14, L11H20, L13H2, L8H9, L7H31
CYBER	1S-GREEDY	L31H14, L13H16, L10H29, L5H19, L7H16
CYBER	CS_B	L11H14, L7H31, L13H16, L15H7, L8H23
CYBER	CS_S	L31H14, L24H14, L27H6, L11H0, L27H13

Table 10. Task-specific heads identified across various tasks and models. All heads are found using stratified compressed sensing.

TASK	HEADS (TOP 5)
	LLAMA 3.2 3B
GSM8K	L16H22, L14H10, L8H8, L12H1, L18H5
ARITHMETIC	L16H22, L14H10, L8H15, L11H19, L25H12
MBPP	L4H6, L17H11, L1H16, L3H20, L0H16
SWEARING	L22H12, L0H2, L1H6, L5H0, L9H11
RHYMING	L16H3, L18H19, L0H0, L0H4, L18H2
WMDP BIO	L10H26, L12H22, L9H9, L21H26, L29H2
WMDP CHEM	L0H24, L0H3, L20H14, L7H21, L18H30
WMDP CYBER	L31H14, L24H14, L27H6, L11H0, L27H13
	LLAMA 3.2 1B
GSM8K	L15H30, L8H30, L5H12, L6H5, L5H3
ARITHMETIC	L11H15, L11H13, L3H6, L11H14, L9H23
MBPP	L3H25, L8H31, L2H27, L10H4, L8H12
SWEARING	L7H14, L15H14, L6H29, L0H2, L9H1
RHYMING	L5H7, L9H2, L9H27, L5H19, L4H31
WMDP BIO	L0H22, L11H8, L2H2, L15H22, L9H26
WMDP CHEM	L0H22, L9H26, L0H4, L11H25, L10H26
WMDP CYBER	L0H22, L6H31, L6H16, L7H28, L5H22
	QWEN 2.5 3B
GSM8K	L27H6, L27H0, L27H1, L18H9, L20H10
MBPP	L0H2, L8H11, L33H11, L0H12, L23H4
SWEARING	L21H10, L17H13, L17H11, L13H0, L30H6
RHYMING	L32H7, L28H11, L4H5, L15H15, L26H9
	QWEN 2.5 7B
GSM8K	L0H0, L0H15, L20H6, L0H25, L1H20
MBPP	L17H13, L19H0, L8H17, L0H23, L11H0
SWEARING	L18H17, L16H8, L7H26, L15H8, L27H14
RHYMING	L0H24, L0H25, L14H16, L25H8, L0H1